Effectiveness of Adaptive Shape Prediction Model for Cytological Cell Segmentation

Afaf Omar Tareef
Faculty of Information Technology, Mutah University, Karak, Jordan

***Abstract*—Cell segmentation continues to be a significant challenge in medical image processing, as traditional segmentation methods fail to provide precise and thorough segmentation of complex structures such as touching and overlapping cells. The geometric data points of these cells are inadequate for accurate contour estimation to yield a correct segmentation. Adaptive shape priors have demonstrated efficacy as a promising solution in these challenging circumstances. They can be employed to restrict segmentation models in medical imaging and enhance segmentation robustness in the presence of a complex structure of touched and overlapped cells. In this study, Adaptive Shape Prior Model (ASPM) is introduced and evaluated using three cervical cell datasets, where all their images have a varied number of cells with different properties, such as texture and degrees of overlap. The segmentation performance of ASPM demonstrates that the contour/shape based deformation procedure yields good segmentation accuracy and can be successfully adapted to numerous cytology images. Compared to the other segmentation models for overlapping cells in the literature, the proposed ASPM offers quicker with more precise segmentation for highly overlapped cells in different cervical images without extensive modifications. These results imply that the proposed ASPM approach is a promising choice for integration into a fully automated cervical cancer screening system.**

***Keywords*—Cytology image; shape prediction model; shape priors; overlapping cell segmentation**

I. Introduction

Cytology, the study of cells under a microscope, is essential to identify numerous diseases, including cancer. The examination of cytology images involves precise cell segmentation to discern individual cells, their structures and characteristics, and any abnormalities [1]. Although automated image analysis has seen advancements owing to deep learning and computer vision techniques, a major hurdle remains, i.e., correct segmentation of nuclei and cytoplasm border, especially in the case of touched and overlapped cells [2]. Usually, both traditional image processing and deep learning segmentation methods face limitations in these challenging scenarios due to several reasons, such as variability in cell morphology, staining inconsistencies, overlapping sections, and low contrast and fuzzy boundaries.

Segmenting cells that are touching or overlapping presents a variety of challenges. Specifically, cells can have a variety of shapes and sizes, making it difficult to generalize and apply the same segmentation rules. Additionally, touching and overlapping cells in cytology images have ambiguous and unclear boundaries, limiting the segmentation effectiveness of edge-based techniques. Predefined constraints regarding the expected shape of the cell, i.e., shape priors, have emerged as a potential way to improve segmentation accuracy by using prior knowledge of cell shapes in similar kinds of cytology images. The literature review in this research will discuss the development of using shape priors in cell segmentation, and discuss the challenges facing an accurate cell segmentation in cytology images.

Regardless of the considerable development in automatic nuclei and cytoplasm delineation techniques, obstacles remain in in precisely and effectively identifying massive, irregularly shaped cells from histopathological images. The advancement of deep learning models, such as CNNs, has made a path to the replacement of traditional segmentation models owing to their optimized features extraction capabilities and accurate outcomes, especially if incorporated with a shape prior knowledge. However, accurate overlapping cell segmentation across diverse kinds of microscopic images under varying circumstances is still unavailable. This research presents both shape-prior based and deep learning models used for segmenting overlapping cells in cervical images since the problem was first introduced by Lu et. al [3] in 2013.

The exchange between computational efficiency and segmentation still stands as a critical thought of mater. Traditional ways are computationally efficient but they do not have the ability to overcome challenging problems, while deep learning models provide better accuracy and generalizability at the price of higher time complexity. Modern enhancements, e.g., C-UNet and TSFD, aim to innovate computational precision. These techniques focus on useful features and ignore non useful ones, bridging the gap between computational productivity and accuracy. The comparative analysis points out the necessity for a balanced model that takes the variations of dataset features and computing constraints into account.

Recently, it becomes well-known that the deep learning segmentation models are the most successful models. However, accurate cell segmentation in histopathological images by deep learning faces many challenges, which can be summarized as follows:

A. Cell Overlapping

Cellular overlap is a common in microscopy images. Cell overlap in Pap smear images commonly come from solidly compressed tissue cell, excessive and messy staining, and bad handling with the sample during slide preparation. The successful determination of cell border is necessary for cancer diagnosis. However, the automatic segmentation methods often confound clustered cells as individual cells, making a path to the deficit of necessary diagnostic information.

B. Preprocessing and Postprocessing

Preprocessing, including resizing, improving, zooming, rotation, etc, is essential step and impact the performance of the automatic segmentation techniques. An equally important step is post-processing especially is the initial segmentation generated by these methods is not instantly appropriate for visualization and medical diagnostic analysis. These two steps add extra loads on designing successful segmentation models.

C. Parameter Adjustment and Generalizability

One of the most challenge facing the traditional image segmentation is parameter tuning and adjustments, which is both exhausting and a massive time waste. Manual selection of parameter values (i.e., thresholds, iterations, smoothing factors, and so on) is a very complicated and such trial-and-error task, which usually requires significant computational resources. Moreover, parameter configuration that is suitable for one dataset could fail on other datasets, restricting the generalizability of the existing segmentation methods. There is still a major need for more flexible and well-generalized approaches that can be efficiently used for cytological analysis.

D. Imaging Inconsistencies

The presence of cancer in histopathological images can be usually detected based on the variation in cell texture, size, and shape. Inconsistencies in imaging parameters such as resolution, bright, contrast, illumination and focus can be resulted in similar variations that are associated with cancer, leading to potential misdiagnosis by pathologists and computerized image segmentation methods.

E. Computational Complexity

Since cytology image datasets are usually large and with high-resolution, employing deep learning in segmentation are computationally intensive and need efficient hardware resources. In addition to this load, adjusting deep learning parameters is often a time-consuming task, adding additional complexity to the segmentation challenge.

F. Lack and Imbalance of Data

It is known that effective deep learning model needs large amounts of data. However, there is sometimes a lack of medical data, especially in cervical cytology images with overlapping cells. In addition, most datasets with overlapping cells were created under controlled conditions that not accurately reflecting real-world clinical settings. Another challenge is class imbalance, in which one class is clearly dominant in the dataset, further affects the model in favour of the majority class leading to a misclassifications. Moreover, the efficiency of the deep learning-based models depends on the quality of the manual annotation of the ground truth, which is time-consuming and frequently inaccurate tasks.

The proposed ASPM is fast and efficient model that does not require extensive parameter tuning, pre-processing/ post-processing steps, or pre-knowledge from training dataset. Thus, ASPM can help with fast and accurate analyses and enable real-time diagnoses, leading to detect cancer in its early stages and decrease the need for invasive treatments. This research study help in understanding current problems with the cervical cell segmentation and its provides insights on the problem for future research paths.

The rest of study is arranged as follows: In Section II, the literature review is presented. The Adaptive Shape Prediction Model (ASPM) is illustrated in details in Section III. The evaluation metrics, results, and discussion are shown in Section IV. Section V concludes with findings and recommendations for future work.

II. Literature Review

As a result of noise, occlusions, and variations in cell morphology, traditional segmentation methods cannot be effectively used for cytology cells. Incorporating shape priors can help address these challenges. With the inclusion of prior information on typical cell shape, the final segmentation produced is more reasonable and accurate. For example, Phoulady et al. [4] introduced a segmentation approach based on an elliptic shape prior, and which was then improved by Nosrati et al. [5] by utilizing a regularized level set evolution with an elliptical shape presumption to get better segmentation results. This method was further improved in [6] by substituting the original elliptic shape-prior with a star shape-prior, which better models cells than traditional elliptical priors. The elliptical shape assumption was also utilized in many segmentation methods such as [3], with a variational method. In [7], Lu et al. proposed another level set model with a geodesic-based shape prior, improving segmentation accuracy for occluded and noisy images.

A different shape-prior segmentation technique is introduced in [8] for separating touching and overlapping cells with complex structure from cytology images. This is achieved by integrating various geometrical and appearance cues, such as shape, color, texture, and shape prior, into an objective function optimized using a tribe-based genetic algorithm for addressing the spatially recurring nature of cell segmentation. Weigert et al. [9] introduced a method using star-convex polyhedra to represent cell nuclei, allowing for more accurate segmentation in 3D fluorescence images. This approach demonstrates the potential of advanced shape representations in handling complex cell structures.

These shape-prior-based methods show good segmentation performance for nuclei and cells in cytology images. Nevertheless, most of the existing shape-prior-based methods consider standard and basic structured shapes prior, disregarding the complex structure of cell shape in cytology images. Therefore, many methods incorporate shape prior with neural networks to get more accurate separation. In the past few years, machine and deep learning has emerged as the leading mechanism for overlapping cell segmentation due to its high efficiency and accurate results, such as [10], [11], [12], [13], [14], [15], [16], [17], [18], [19]. In [12], [13] a dynamically learned shape is incorporated with a deformation model to construct cytoplasm shapes for each cell. Firstly, machine learning methods were employed based on different shape and appearance cues to segment the image into its main components, i.e., nucleus, clusters, and background. Then, a shape deformation model driven by shape cues was utilized in order to estimate the border of each cell. Nevertheless, deep learning is considered

a complex and computationally intensive technique that relies heavily on the availability of large amounts of training images. Other models to segment overlapping cell in cervical images try to approximate the overlapped cells based on their edge information, e.g., [20], [21], [22], [23], [24], [25], [26]. However, edge points are usually ambiguous and unclear in highly overlapped cells and depending on these points only without references or shape priors leads to inaccurate segmentation. Overall, correct segmentation of overlapping cells in cervical images is still an open and active research challenge with ongoing efforts to achieve a satisfactory segmentation performance with an acceptable time complexity, that enables the design of fully automated diagnostic systems employed in real-world medical and technological sectors.

III. Adaptive Shape Prediction Model (ASPM)

The idea for the designed ASPM evolved from the shape-learning segmentation method [12], while being simpler and computationally faster with maintaining comparable performance. In addition, ASPM is able to generalize to different kinds of cytology images with extensive training or parameters tuning procedures. This research shows the effectiveness of ASPM in predicting the cell cytoplasm in the cellular mass using the cluster boundaries and elliptical shape knowledge without pre-training. This adaptable shape deformation model iteratively alternates between two steps until a satisfactory cell segmentation is obtained, which are Cell-wise contour-based deformation and reference shaped-based deformation.

A. Nuclei and Cellular Clump Segmentation

The nuclei and cellular clumps are first separated in order to assess the effectiveness of the proposed ASPM. In this work, the cellular clump is extracted using the triangle algorithm, which constructs a line between the histogram peak and the farthest point, then finds the maximum perpendicular distance. Then, the edge artifacts is eliminated, and small connected components (area ¡ 100 pixels) are removed to obtain an acceptable cellular clump.

For nuclei localization, Maximally Stable Extremal Regions (MSER) [27] combined with morphological refinement and level set segmentation are performed. This process starts by image smoothing with a larger Gaussian kernel ($\Sigma = 10$) to enhance blob-like structures. Then, MSER is applied and the inappropriate blobs (i.e., with very small or large size or high eccentricity) are filtered out. To further refine nuclei boundaries and remove residual noise, an active contour model is applied. The level set evolution smooths boundaries and eliminates small irregularities that survived the geometric filtering.

B. Cell-Wise Contour-Based Deformation

The contour initialization process is known to have a significant impact on the efficiency of segmentation models. Thus, the contour deformation process is started with employing an initially predetermined cell diameter that originates from the cell nucleus to determine a closed circular region-of-interest (ROI). This cell diameter is iteratively modified based on the landmark points, which are the outer edge points between the cell and background and positioned inside the ROI for each cell. For initial segmentation, Triangle thresholding [28] is firstly applied on the cellular mass. Then, the cell located within the ROI is retrieved as initial cell mask. To prove the effectiveness of ASPM, Voronoi diagram [29] can be employed as an option for initial cell segmentation. The next step is the cell-wise prediction process starting with a landmark points, and predict the next points as shown in Fig. 1.

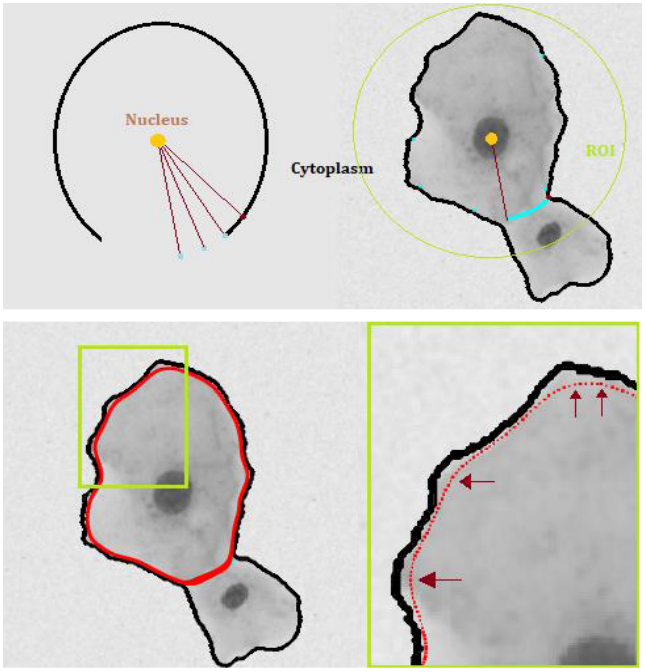

Fig. 1. The first row is the cell-wise contour based deformation procedure, where the black contour shows the landmarks of the whole cellular mass, the red contour shows the cell landmarks used to generate the missed points to complete the cell-in-focus shape. The second row represents the reference shape deformation, where the red contour shows the cell shape after the reference based deformation procedure. During the smoothing process, some landmarks are shifted, therefore, they are restored to their original coordinates at the end of each deformation iteration.

As cytology images usually contain highly overlapping cells, this make it impossible for any automatic method to distinguish, with absolute certainty, between the boundaries belonging to each overlapped cell. Thus, ASPM deals with this point by calculating the radius difference between the last confirmed landmark point belonging to the cell and the new point; if this distance is less than a specific threshold value, the new point is adopted as part of the cell-in-focus boundary; otherwise, the distance of the previous confirmed point is used to generate a new point connected to the preceding one. Finally, cell contour linking is accomplished using morphological operations (i.e., closing and dilating the contour after deleting the isolated pixels) in order to obtain distinct and connected edges that closely mimic the cell shape.

C. Reference Shape-Based Deformation

The proposed ASPM predicts the cell shape based on two parameters: the cell landmarks located between the cell and background, and the reference shape, which is typically an elliptical cell shape. The ASPM starts by Looping until finding the first landmarks points in order to strat generating the input shape from feature points to get more accurate shape

establishment. Then, ASPM starts predicting the missed points connected to the landmark points and located with the updated ROI. After that, a reference-based deformation is applied on the output shape in order to make it more similar to the reference shape and smoothen the shape using the Procrustes transformation [30].

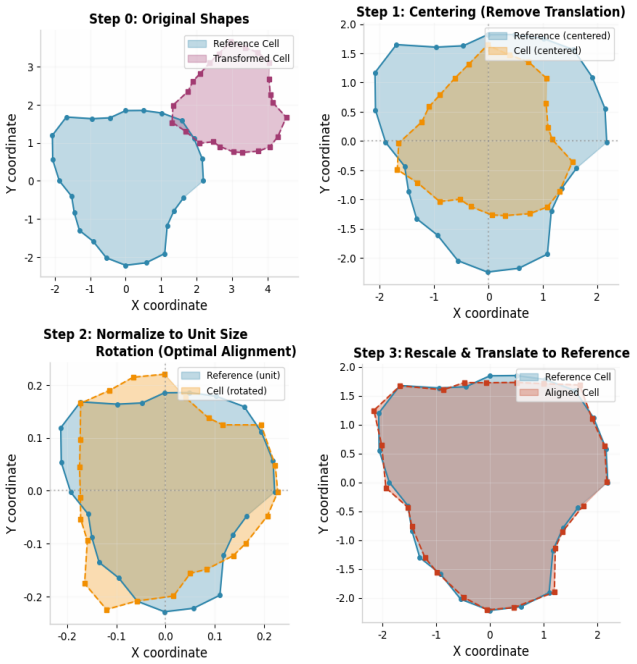

Fig. 2. The Procrustes analysis steps performed to align a given cell shape to a reference shape (blue). Both shapes are centered at the origin to remove translation differences, then they are normalized to unit size and rotates to remove scale differences and optimally align with the reference using SVD. Finally, The given cell is rescaled back to the reference size and translated to the reference position, resulting in near-perfect overlap.

The Procrustes analysis, also known as Procrustes transformation or Procrustes superimposition, is a statistical shape analysis technique utilized to align two or more points by diminishing the total of squared differences between the corresponding points in order to optimally estimate the similarity transformation, which includes rotation, reflection, uniform scaling, and translation. Fig. 2 illustrates the steps of Procrustes analysis to align a given cell shape to a reference shape, which should be one-to-one point correspondence: first, the centroid of each shape are calculated. After that, they are re-scaled and rotated to have equal size and similar orientation.

The process of reference-based deformation of ASPM involves two processes: the input cell shape is first adjusted to match the reference cell shape by the previous steps of Procrustes analysis, and then the following equation is used to transform the resulting shape points back to the input shape domain, as follows:

$$Cell_O = \frac{(Cell_P - T) \times R^{-1}}{S} \tag{1}$$

where, the translation part is denoted by T, the inverse rotation part by R^{-1}, and the scale part by S. It is often noted that the resulting shape tends to take on an oval shape, which inadvertently alters some landmarks coordinates, and thereby distorts the original morphological characteristics that are essential for accurate segmentation (as illustrated in the right image of Fig. 1). This bias emerges as an unintended consequence of the standard Procrustes superimposition process, wherein the optimization algorithm prioritizes the minimization of global squared distances between the points. To address this issue, the landmark points are restored to their original coordinates at the end of each deformation process. This corrective step is strategically formulated to preserve the distinctive shape information that characterizes the unique architecture of each individual cell. Simultaneously, this re-transformation maintains the capacity to appropriately handle the natural shape variation present across the sample population, thereby achieving a balance between geometric standardization and the morphological information of each cell.

Subsequently, the transformed shape coordinates already undergone the requisite re-transformation procedure to preserve their distinctive morphological characteristics are subsequently subjected to an additional smoothing operation by employing a low-pass moving average filter [31], which is a kind of Finite Impulse Response (FIR) filter performed to smooth data by creating an average of different subsets of the full data. This deliberate post-processing step serves the critical purpose of discerning and reinforcing the underlying shape connectivity and regularity. This smoothing procedure are formally articulated in the equations Eq. (2), which are explicitly developed for the first few elements of the coordinate sequence [see Eq. (3)] to exemplify the recursive averaging pattern and illustrate the progressive regularization of the transformed boundary coordinates.

$$p_t(n) = \frac{p(n-2) + p(n-1) + p(n) + p(n+1) + p(n+2)}{5} \tag{2}$$

$$\begin{aligned} p_t(1) &= p(1) \\ p_t(2) &= (p(1) + p(2) + p(3))/3 \\ p_t(3) &= (p(1) + p(2) + p(3) + p(4) + p(5))/5 \\ p_t(4) &= (p(2) + p(3) + p(4) + p(5) + p(6))/5 \end{aligned} \tag{3}$$

where, p_t denotes the smoothed coordinate at position n, and $p(n)$ represents the original transformed coordinate, with the window size adaptively expanding at the sequence boundaries to accommodate the finite extent of the landmarks while maintaining computational consistency across the entire contour.

Finally, the size of the predicted cytoplasm candidates are checked to filter out those that are too small or too large to be considered cells.

IV. Results and Discussion

The precise segmentation system for cytology images stand as a journey of problem because of the complexity of cell structures resulting from the existence of blood, mucus, and inflammation-related cells, and a high overlapping degree.

The power of ASPM lies in its efficiency and flexibility in separation of the touched and overlapped cells in various kinds of cytology images regardless the image texture or intensities.The suggested ASPM depends entirely on the cell clump border, which can be simply identified using many strategies in the literature.

A. Evaluation Metrics

The nuclei segmentation evaluation is performed by calculating the object based precision ($prec_o$) and recall (rec_o), the pixel based precision ($prec_p$) and recall (rec_p) for the good segmentation of nuclei, meeting the standards set by Gençtav et al. [32] and defined as follows:

$$\frac{N_{Sg} \cap N_{GT}}{N_{Sg}} > 0.6 \quad \text{and} \quad \frac{N_{Sg} \cap N_{GT}}{N_{GT}} > 0.6 \tag{4}$$

where, N_{GT} stands for the ground truth nuclei used to classify all segmented nuclei (N_{Sg}) into true positive O_{TP}, false positive N_{FP}, or false negative N_{FN} objects. The numbers of true positive pixels (TP), false positive pixels (FP), and false negative pixels (FN) were also computed for each true detection N_{TP}. The performance measures are thus defined as follows, where $\#$ denotes the number of objects:

$$prec_o = \frac{\text{Correctly Segmented Nuclei}}{\sum \text{All Segmented Nuclei}} = \frac{\#N_{TP}}{\#N_{Sg}} \tag{5}$$

$$rec_o = \frac{\sum \text{Correctly Segmented Nuclei}}{\sum \text{All GT Nuclei}} = \frac{\#N_{TP}}{\#N_{Gt}} \tag{6}$$

$$prec_p = \frac{\sum \text{Correctly Segmented Pixels}}{\sum \text{All Segmented Pixels}} = \frac{TP}{TP + FP} \tag{7}$$

$$rec_p = \frac{\sum \text{Correctly Segmented Pixels}}{\sum \text{All GT Pixels}} = \frac{TP}{TP + FN} \tag{8}$$

For cell quantitative assessment, true positive rate (TP_p), and false positive rate (FP_p), the object-level false negative (FN_O), and the Zijdenbos similarity index (ZSI), also known as the Dice similarity coefficient, are computed in the evaluation by the following equations:

$$DC = 2\ \frac{|O_{GT} \cap O_{Sg}|}{|O_{GT}| + |O_{Sg}|} \tag{9}$$

where, O_{GT} is the ground truth cell object, O_{Sg} is the segmented one by ASPM, and $|.|$ denotes the number of pixels in the region. The TP_p, FP_p were computed for a 'good'cell segmentation with ZSI higher than 0.7 [33], and FN_o for remaining cell segmentation by the following equations:

$$TP_p = \frac{\sum \text{Correctly Segmented Pixels}}{\sum \text{All Segmented Pixels}} = \frac{TP}{TP + FP} \tag{10}$$

$$FP_p = \frac{\sum \text{Missed Pixels}}{\sum \text{All Segmented Pixels}} = \frac{FP}{TP + FP} \tag{11}$$

$$FN_o = \frac{\text{Number of Missed Objects}}{\text{Number of GT Objects}} = \frac{\#O_{GT} - \#O_{TP}}{\#O_{GT}} \tag{12}$$

TABLE I. THE PERFORMANCE RESULTS OF THE NUCLEI SEGMENTATION, REPRESENTED BY THE MEAN AND STANDARD DEVIATION OF EACH MEASURE

Methods	$Prec_O$	Rec_O	$Prec_P$	Rec_P
[34]	0.96	0.90	0.97 (±0.06)	0.87 (±0.07)
[5]	0.90	0.89	0.90 (±0.10)	0.92 (±0.09)
[7]	0.98	0.88	0.94 (±0.08)	0.91 (±0.08)
[35]	0.99	0.96	0.94 (±0.03)	0.92 (±0.08)
[36]	0.94	0.96	0.98 (±0.02)	0.90 (±0.09)
[37]	0.97	0.96	0.98 (±0.03)	0.90 (±0.08)
[38]	0.99	0.94	0.95 (±0.06)	0.93 (±0.07)
[13]	0.99	0.91	0.94 (±0.06)	0.95 (±0.06)
[39]	0.98	0.96	0.91 (±0.07)	0.95 (±0.05)
ASPM	0.98	0.98	0.92 (±0.09)	0.95 (±0.08)

B. Image Datasets

For ASPM evaluation, three cervical cell datasets, released by the first and second "ISBI Overlapping Cervical Cytology Image Segmentation Challenge"[40], [41] are used. The first dataset is the synthetic dataset offered by the ISBI challenge organizers [3]. The second dataset is the ISBI 2014 test dataset of 90 synthetic images with size of 512 × 512 pixels and different overlapping degree. The third dataset is the ISBI 2015 with real Extended Depth of Field (EDF) images of size 1024×1024 pixels. All datasets have a varied number of cells with different properties (such as texture and degrees of overlap), and all their images are annotated with the ground truths of both nuclei and cytoplasm.

C. Discussion

The core and importance of this method lies in its generalization for any type of cytology images without extensive parameter tuning, significant modification, or extensive preprocessing or post-processing processes. Also, it can be used as initial segmentation for further complex segmentation. To prove this, the designed method is compared with the state-of-the-art methods. Table I shows the nuclei segmentation results. The proposed ASPM achieves a good results with best Rec_o and Rec_p performance. Table II shows the cytoplasm segmentation results where it is proven that the proposed method achieve a high performance compared to the other methods used in the literature. The ASPM obtains a high ZSI of 0.9 and more on the three datasets. In addition, it yields the highest TP_P on the first and third dataset, and the lowest FP_P on the third dataset. However, the FN_O of the proposed ASPM is higher than some other methods, e.g., Nosrati [5], [6] and Huang [15] on the second dataset due to the insufficient

TABLE II. THE PERFORMANCE RESULTS OF THE CYTOPLASM SEGMENTATION

Methods	ZSI	TP_p	FP_p	FN_o
Test dataset of [3]				
Baseline^a [3]	0.88 (±0.08)	0.92 (±0.10)	0.002 (±0.005)	0.21 (±0.29)
Tareef [35]	0.91 (±0.08)	0.95 (±0.06)	0.004 (±0.012)	0.24 (±0.24)
Tareef [36]	0.92 (±0.06)	0.94 (±0.05)	0.005 (±0.007)	0.07 (±0.14)
Tareef [37]	0.91 (±0.05)	0.92 (±0.05)	0.005 (±0.010)	0.00 (±0.00)
Tareef [39]	0.93 (±0.06)	0.92 (±0.09)	0.004 (±0.005)	0.00 (±0.00)
ASPM	0.93 (±0.07)	0.95 (±0.08)	0.005 (±0.008)	0.21 (±0.22)
ISBI 2014 test dataset				
Ushizima [34]	0.87 (±0.08)	0.83 (±0.13)	0.001 (±0.002)	0.17 (±0.21)
Nosrati [5]	0.87 (±0.08)	0.90 (±0.09)	0.005 (±0.004)	0.14 (±0.17)
Nosrati [6]	0.88 (±0.08)	0.93 (±0.09)	0.005 (±0.004)	0.11 (±0.17)
Baseline^b [7]	0.89 (±0.08)	0.91 (±0.10)	0.003 (±0.005)	0.32 (±0.29)
Tareef [37]	0.89 (±0.08)	0.94 (±0.07)	0.005 (±0.005)	0.16 (±0.17)
Tareef [12]	0.89 (±0.07)	0.91 (±0.09)	0.004 (±0.005)	0.27 (±0.28)
Tareef [13]	0.90 (±0.08)	0.95 (±0.07)	0.005 (±0.005)	0.22 (±0.24)
Tareef [39]	0.90 (±0.08)	0.95 (±0.07)	0.005 (±0.004)	0.22 (±0.24)
Huang [15]	0.89 (±0.07)	0.94 (±0.09)	0.004 (±0.003)	0.10 (±0.13)
Liu [23]	0.90 (±0.07)	0.91 (±0.09)	0.003 (±0.005)	0.28 (±0.23)
ASPM	0.90 (±0.08)	0.92 (±0.10)	0.004 (±0.006)	0.28 (±0.30)
ISBI 2015 real EDF images				
Lu [7]	0.87 (±0.09)	0.90 (±0.10)	0.00 (±0.00)	0.36 (±0.08)
Ushizima [34]	0.84 (±NA)	0.83 (±NA)	NA	0.47 (±NA)
Phoulady [4]	0.83 (±0.08)	0.93 (±0.10)	0.003 (±0.002)	0.41 (±0.02)
Ramalho [20]	0.86 (±0.08)	0.90 (±0.11)	0.002 (±0.001)	0.50 (±0.02)
Phoulady [10]	0.86 (±NA)	0.87 (±NA)	0.001 (±NA)	0.35 (±NA)
Kumar [21]	0.85 (±0.08)	0.89 (±0.10)	0.002 (±0.001)	0.36 (±0.16)
Lee [22]	0.88 (±0.09)	0.88 (±0.12)	0.001 (±0.001)	0.43 (±0.02)
Song [11]	0.89 (±NA)	0.92 (±NA)	0.002 (±NA)	0.26 (±NA)
Tareef [39]	0.88 (±0.08)	0.92 (±0.08)	0.002 (±0.002)	0.23 (±0.13)
Wan [14]	0.92 (±0.05)	0.91 (±0.05)	0.001 (±0.003)	0.24 (±0.19)
Wang [24]	0.88 (±NA)	0.85 (±NA)	NA	0.32 (±NA)
Zhang [19]	0.88 (±0.03)	0.91 (±0.04)	0.001 (±0.003)	0.20 (±0.11)
ASPM	0.90 (±0.09)	0.94 (±0.09)	0.001 (±0.002)	0.29 (±0.13)

number of cell landmarks used to predict the irregular shape of overlapping cells. These results is significantly enhanced by performing initial segmentation such as Voronoi diagram as suggested in ASPM. The designed ASPM with Voronoi is utilized on the second datasets and it achieves a higher segmentation performance with ZSI of 0.92 (±0.06), TP_P of 0.94 (±0.08), FP_P of 0.003 (±0.003), whereas the FN_O is still 0.28.

Fig. 3 demonstrates these quantitative results, where most of touched and overlapped cell were successfully segmented, compared to other complex methods. However, the ASPM segmentation in Fig. 3 presents some of the failure case of ASPM occurring due to the short distance/radius between the nucleus and the cell landmarks. This limitation could potentially be addressed by generating two or more possible shapes by multiple prediction techniques or by initializing the prediction process from different starting points, followed by the application of the generalized Procrustes analysis [30] to get the best shape prediction, which will be the future work.

The performance of ASPM can be further enhanced by integrating an adaptive shape prior with several segmentation methodologies. The graph-based techniques can be also employed as a post-processing steps in order to enhance border estimation and the distinction between touching and overlapping cells. Nevertheless, this research aims to show the effectiveness of ASPM in its simplest and fastest form to confirm it can efficiently adapt to diverse microscopy image types without exhausting parameter adjustments.

In conclusion, the training-free, parameter-minimal design

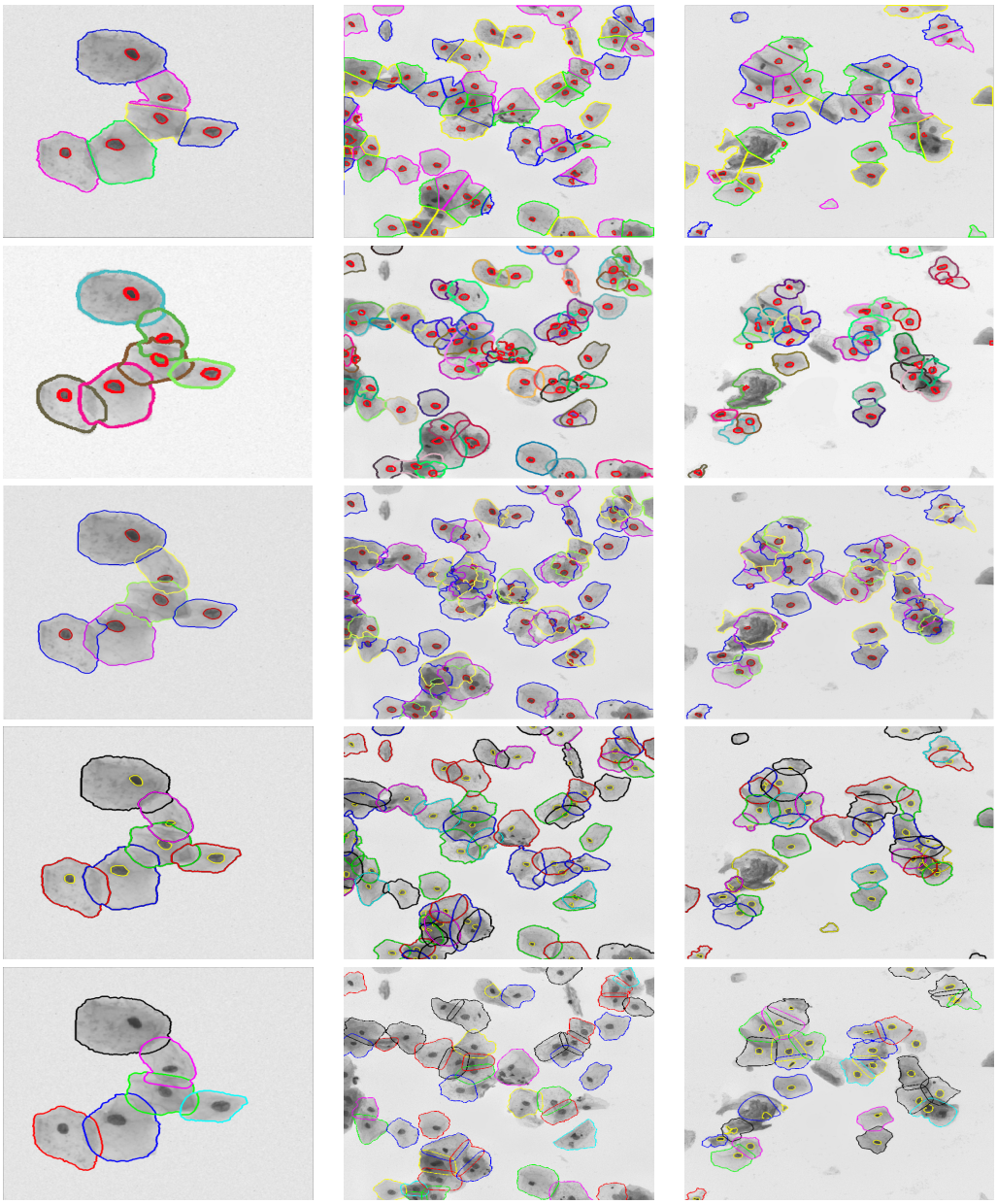

Fig. 3. Visual comparison between the proposed ASPM method and the ISBI-14 challenge methods using the synthetic and real EDF images provided by the challenge report . The first row presents the results of [34], the second one presents the results of [5], the third one presents the results of [2], the fourth one presents the results of [39], and the last row shows the results of the proposed ASPM with initial segmentation.

of ASPM is a genuine practical contribution for cytological screening environments where labeled cell datasets are scarce and re-parameterization for new staining protocols is costly. The successful generalization across three structurally distinct ISBI datasets, including synthetic and real EDF images, supports the portability claim of the designed ASPM.

V. Conclusions

This research aims to improve automated cytological analysis and diagnostic precision by addressing challenges associated with touching and overlapping cells on cytology images. It will demonstrate the effectiveness of adaptive shape prediction for accurate cell segmentation. The designed shape prediction model focuses on developing adaptive, real-time, and explainable shape-based models for biomedical imaging applications by incorporating adaptive edge-based and general elliptical shape prior in touching and overlapping cell segmentation to improve diagnostic accuracy rather than using predefined shape templates.

Regardless of the great performance of ASPM model, it has some failure cases for highly overlapped cells with Inadequate landmarks, or large variation in their size. These issue can be addressed by employing a good initial separation followed by contouring procedures. The proposed ASPM offers quicker with more precise and accurate segmentation strategy for highly overlapped cells that can be also used for diverse

kind of microscopy images without extensive modifications. In addition, the designed ASPM will work perfectly for regular elliptical shape entities such as overlapping nuclei segmentation even if the border between nuclei is not clear.

Code Availability

The simplest version of ASPM for cytoplasm segmentation is available on GitHub via the following link: https://github.com/AfafTareef/ASPM.git.

References

[1] M. A. Al-Abbadi, "Basics of cytology," *Avicenna journal of medicine*, vol. 1, no. 01, pp. 18–28, 2011.

[2] Z. Lu, G. Carneiro, A. Bradley, D. Ushizima, M. S. Nosrati, A. Bianchi, C. Carneiro, and G. Hamarneh, "Evaluation of three algorithms for the segmentation of overlapping cervical cells," *IEEE Journal of Biomedical and Health Informatics*, vol. 21, no. 2, pp. 441–450, 2017.

[3] Z. Lu, G. Carneiro, and A. P. Bradley, "Automated nucleus and cytoplasm segmentation of overlapping cervical cells," in *International Conference on Medical Image Computing and Computer-Assisted Intervention*. Springer, 2013, pp. 452–460.

[4] H. A. Phoulady, D. B. Goldgof, L. O. Hall, and P. R. Mouton, "An approach for overlapping cell segmentation in multi-layer cervical cell volumes," *IEEE ISBI Second Overlapping Cervical Cytology Image Segmentation Challenge*, 2015.

[5] M. Nosrati and G. Hamarneh, "A variational approach for overlapping cell segmentation," in *ISBI Overlapping Cervical Cytology Image Segmentation Challenge*. IEEE, 2014, pp. 1–2.

[6] ——, "Segmentation of overlapping cervical cells: A variational method with star-shape prior," in *International Symposium on Biomedical Imaging (ISBI)*. IEEE, 2015, pp. 186–189.

[7] Z. Lu, G. Carneiro, and A. P. Bradley, "An improved joint optimization of multiple level set functions for the segmentation of overlapping cervical cells," *IEEE Transactions on Image Processing*, vol. 24, no. 4, pp. 1261–1272, 2015.

[8] M. S. Nosrati and G. Hamarneh, "Segmentation of cells with partial occlusion and part configuration constraint using evolutionary computation," in *Medical Image Computing and Computer-Assisted Intervention*. Springer, 2013, pp. 461–468.

[9] M. Weigert, U. Schmidt, R. Haase, K. Sugawara, and G. Myers, "Star-convex polyhedra for 3d object detection and segmentation in microscopy," in *Proceedings of the IEEE/CVF winter conference on applications of computer vision*, 2020, pp. 3666–3673.

[10] H. Phoulady, D. Goldgof, L. Hall, and P. Mouton, "A new approach to detect and segment overlapping cells in multi-layer cervical cell volume images," in *International Symposium on Biomedical Imaging (ISBI)*. IEEE, 2016, pp. 201–204.

[11] Y. Song, E.-L. Tan, X. Jiang, J.-Z. Cheng, D. Ni, S. Chen, B. Lei, and T. Wang, "Accurate cervical cell segmentation from overlapping clumps in pap smear images," *IEEE transactions on medical imaging*, vol. 36, no. 1, pp. 288–300, 2016.

[12] A. Tareef, Y. Song, W. Cai, H. Huang, H. Chang, Y. Wang, M. Fulham, D. Feng, and M. Chen, "Automatic segmentation of overlapping cervical smear cells based on local distinctive features and guided shape deformation," *Neurocomputing*, vol. 221, pp. 94–107, 2017.

[13] A. Tareef, Y. Song, H. Huang, Y. Wang, D. Feng, M. Chen, and W. Cai, "Optimizing the cervix cytological examination based on deep learning and dynamic shape modeling," *Neurocomputing*, vol. 248, pp. 28–40, 2017.

[14] T. Wan, S. Xu, C. Sang, Y. Jin, and Z. Qin, "Accurate segmentation of overlapping cells in cervical cytology with deep convolutional neural networks," *Neurocomputing*, vol. 365, pp. 157–170, 2019.

[15] Y. Huang, H. Zhu, P. Wang, and D. Dong, "Segmentation of overlapping cervical smear cells based on u-net and improved level set," in *2019 IEEE International Conference on Systems, Man and Cybernetics (SMC)*. IEEE, 2019, pp. 3031–3035.

[16] H. Jiang, R. Zhang, Y. Zhou, Y. Wang, and H. Chen, "Donet: Deep de-overlapping network for cytology instance segmentation," in *Proceedings of the IEEE/CVF conference on computer vision and pattern recognition*, 2023, pp. 15 641–15 650.

[17] L. Li, W. Chen, and J. Qi, "Vb-solo: Single-stage instance segmentation of overlapping epithelial cells," *IEEE Access*, vol. 12, pp. 52 555–52 564, 2024.

[18] V. M. K. Nguyen, K. N. V. Ngoc, V. Vu, T. Nguyen, T.-H. Nguyen, and M. Xu, "Beyond visible boundaries: Benchmarking foundation models for overlapping cell segmentation in microscopic imaging," 2026.

[19] B. Zhang, W. Zhao, C. Huang, Q. Lan, and W. Lu, "Optimized segmentation of overlapping cervical cells based on mask2former and denoising," *Scientific Reports*, vol. 15, no. 1, p. 17715, 2025.

[20] G. L. Ramalho, D. S. Ferreira, A. G. Bianchi, C. M. Carneiro, F. N. Medeiros, and D. M. Ushizima, "Cell reconstruction under voronoi and enclosing ellipses from 3D microscopy," *IEEE ISBI Overlapping Cervical Cytology Image Segmentation Challenge*, pp. 3–4, 2015.

[21] P. Kumar, S. Happy, S. Chatterjee, D. Sheet, and A. Routray, "An unsupervised approach for overlapping cervical cell cytoplasm segmentation," in *IEEE EMBS Conference on Biomedical Engineering and Sciences (IECBES)*. IEEE, 2016, pp. 106–109.

[22] H. Lee and J. Kim, "Segmentation of overlapping cervical cells in microscopic images with superpixel partitioning and cell-wise contour refinement," in *Proceedings of the IEEE conference on computer vision and pattern recognition workshops*, 2016, pp. 63–69.

[23] G. Liu, Q. Ding, H. Luo, M. Ju, T. Jin, M. He, and G. Dong, "A novel evolution strategy of level set method for the segmentation of overlapping cervical cells," *Applied sciences*, vol. 11, no. 1, p. 443, 2021.

[24] T. Wang, H. Lan, L. Niu, Z. Fan, and G. Yang, "Overlapping cell segmentation of cervical cytology images based on nuclear radial boundary enhancement," *Mobile Information Systems*, vol. 2022, no. 1, p. 5969056, 2022.

[25] T. Wang, "Overlapping cell segmentation with depth," in *The 8th International Conference on Advanced Machine Learning and Technologies and Applications (AMLTA2022)*. Springer Nature, 2022, p. 278.

[26] F. Zhang, Y. Wu, M. Xu, S. Liu, C. Peng, and Z. Gao, "A morphological image segmentation algorithm for circular overlapping cells." *Intelligent Automation & Soft Computing*, vol. 32, no. 1, 2022.

[27] J. Matas, O. Chum, M. Urban, and T. Pajdla, "Robust wide-baseline stereo from maximally stable extremal regions," *Image and vision computing*, vol. 22, no. 10, pp. 761–767, 2004.

[28] G. Zack, W. Rogers, and S. Latt, "Automatic measurement of sister chromatid exchange frequency." *Journal of Histochemistry & Cytochemistry*, vol. 25, no. 7, pp. 741–753, 1977.

[29] T. Fu, X. Yin, and Y. Zhang, "Voronoi algorithm model and the realization of its program," *Computer Simulation*, vol. 23, no. 10, pp. 89–91, 2006.

[30] J. C. Gower, "Generalized procrustes analysis," *Psychometrika*, vol. 40, no. 1, pp. 33–51, 1975.

[31] J. L. Guiñón, E. Ortega, J. García-Antón, and V. Pérez-Herranz, "Moving average and savitzki-golay smoothing filters using mathcad," *Papers ICEE*, vol. 2007, pp. 1–4, 2007.

[32] A. Gençtav, S. Aksoy, and S. Önder, "Unsupervised segmentation and classification of cervical cell images," *Pattern Recognition*, vol. 45, no. 12, pp. 4151–4168, 2012.

[33] P. Radau, Y. Lu, K. Connelly, G. Paul, A. Dick, and G. Wright, "Evaluation framework for algorithms segmenting short axis cardiac mri," *The MIDAS Journal-Cardiac MR Left Ventricle Segmentation Challenge*, vol. 49, 2009.

[34] D. Ushizima, A. Bianch, and C. Carneiro, "Segmentation of subcellular compartiments combining superpixel representation with voronoi diagrams," in *ISBI Overlapping Cervical Cytology Image Segmentation Challenge*. IEEE, 2014, pp. 1–2.

[35] A. Tareef, Y. Song, W. Cai, D. Feng, and M. Chen, "Automated three-stage nucleus and cytoplasm segmentation of overlapping cells," in *Control Automation Robotics & Vision (ICARCV), 2014 13th International Conference on*. IEEE, 2014, pp. 865–870.

[36] A. Tareef, Y. Song, M.-Z. Lee, D. D. Feng, M. Chen, and W. Cai, "Morphological filtering and hierarchical deformation for partially overlapping cell segmentation," in *International Conference on Digital Image Computing: Techniques and Applications (DICTA)*. IEEE, 2015, pp. 1–7.

[37] A. Tareef, Y. Song, W. Cai, H. Huang, Y. Wang, D. Feng, and M. Chen, "Learning shape-driven segmentation based on neural network and sparse reconstruction toward automated cell analysis of cervical smears," in *Neural Information Processing*. Springer, 2015, pp. 390–400.

[38] A. Tareef, Y. Song, W. Cai, Y. Wang, D. Feng, and M. Chen, "Automatic nuclei and cytoplasm segmentation of leukocytes with color and texture-based image enhancement," in *ISBI*. IEEE, 2016, pp. 935–938.

[39] A. Tareef, Y. Song, H. Huang, D. Feng, M. Chen, Y. Wang, and W. Cai, "Multi-pass fast watershed for accurate segmentation of overlapping cervical cells," *IEEE transactions on medical imaging*, vol. 37, no. 9, pp. 2044–2059, 2018.

[40] Overlapping Cervical Cytology Image Segmentation Challenge ISBI 2014, http://cs.adelaide.edu.au/ carneiro/isbi14_challenge/.

[41] Second Overlapping Cervical Cytology Image Segmentation Challenge-ISBI 2015, http://cs.adelaide.edu.au/ zhi/isbi15_challenge/.